p53 Prohibits Propagation of Chromosome Segregation Errors that Produce Structural Aneuploidies

Soto, Mar; Raaijmakers, Jonne A; Bakker, Bjorn; Spierings, Diana; Lansdorp, Peter; Foijer, Floris; Medema, René H

Published in:
Cell reports

DOI:
10.1016/j.celrep.2017.05.055

Publication date:
2017

Report

Cell Reports

p53 Prohibits Propagation of Chromosome Segregation Errors that Produce Structural Aneuploidies

Graphical Abstract

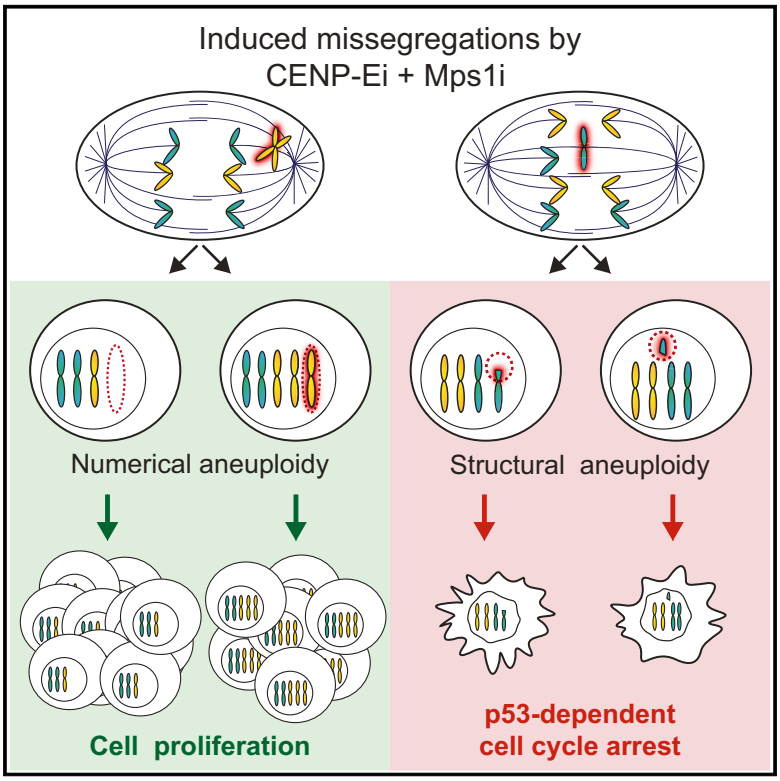

Authors

Mar Soto, Jonne A. Raaijmakers, Bjorn Bakker, Diana C.J. Spierings, Peter M. Lansdorp, Floris Foijer, René H. Medema

Correspondence

r.medema@nki.nl

In Brief

Chromosome segregation errors can result in whole-chromosome aneuploidies or structural aneuploidies (involving only chromosome fragments). Here, Soto et al. show that whole-chromosome aneuploidies do not always lead to p53 activation and can therefore be propagated in a p53-proficient setting, whereas structural imbalances that result from segregation errors cannot.

Highlights

- Whole-chromosome aneuploidy does not invariably lead to p53 activation
- Propagation of structural aneuploidies is limited to p53-deficient cells

Soto et al., 2017, Cell Reports *19*, 2423–2431
June 20, 2017
http://dx.doi.org/10.1016/j.celrep.2017.05.055

Cell Reports
Report

p53 Prohibits Propagation of Chromosome Segregation Errors that Produce Structural Aneuploidies

Mar Soto,[1,3] Jonne A. Raaijmakers,[1,3] Bjorn Bakker,[2] Diana C.J. Spierings,[2] Peter M. Lansdorp,[2] Floris Foijer,[2] and René H. Medema[1,4,*]

[1]Department of Cell Biology and Cancer Genomics Center, Netherlands Cancer Institute, Plesmanlaan 121, 1066 CX Amsterdam, the Netherlands

[2]European Research Institute for the Biology of Ageing, University of Groningen, University Medical Center Groningen, A. Deusinglaan 1, Groningen 9713 AV, the Netherlands

[3]These authors contributed equally

[4]Lead Contact

*Correspondence: r.medema@nki.nl

http://dx.doi.org/10.1016/j.celrep.2017.05.055

SUMMARY

The presence of an abnormal karyotype has been shown to be profoundly detrimental at the cellular and organismal levels but is an overt hallmark of cancer. Aneuploidy can lead to p53 activation and thereby prevents proliferation, but the exact trigger for p53 activation has remained controversial. Here, we have used a system to induce aneuploidy in untransformed human cells to explore how cells deal with different segregation errors. We show that p53 is activated only in a subset of the cells with altered chromosome content. Importantly, we find that at least a subset of whole-chromosome aneuploidies can be propagated in p53-proficient cells, indicating that aneuploidy does not always lead to activation of p53. Finally, we demonstrate that propagation of structural aneuploidies (gain or loss of part of a chromosome) induced by segregation errors is limited to p53-deficient cells.

INTRODUCTION

Segregation of chromosomes is known to fail occasionally in normal cells and more frequently in cancer cells, resulting in offspring that inherit a different complement of chromosomes, a state that is referred to as aneuploidy (Holland and Cleveland, 2009). Aneuploidy has been shown to be profoundly detrimental at both the cellular and organismal levels in all species tested to date (Gordon et al., 2012). One profound consequence of aneuploidy, originally observed in fibroblasts of Down syndrome patients, is their impaired proliferative capacity (Segal and McCoy, 1974). This phenotype is now well described for different species, such as yeast (Torres et al., 2007) and mice (Williams et al., 2008). The proliferative disadvantage might be explained in several ways, as aneuploid cells exhibit a variety of stress-related phenotypes (Tang et al., 2011; Torres et al., 2007).

Aneuploidy can lead to activation of p53 (Santaguida and Amon, 2015), but how p53 activation is triggered in response to aneuploidy has remained a controversial matter. It has been proposed that aneuploidy per se can activate p53 either through the p38 stress kinase (Thompson and Compton, 2010) or because of elevated levels of DNA damage induced by increased production of reactive oxygen species (Li et al., 2010). Alternatively, chromosome segregation errors were shown to produce DNA breaks that activate p53 through the activation of ATM (Janssen et al., 2011). Finally, an increased mitotic duration, which is often associated with erroneous chromosome segregation, can induce p53 via a p38-dependent pathway (Uetake and Sluder, 2010). To understand how abnormal karyotypes can arise and be propagated, we need a better appreciation of the direct consequences of de novo aneuploidy on p53 activation.

Here, we have induced de novo aneuploidies in non-transformed retinal pigment epithelial (RPE-1) cells in both p53-proficient and p53-deficient backgrounds. Interestingly, we find that p53 is not always activated in response to induced aneuploidy, arguing that p53 is not inevitably activated by aneuploidy per se. Importantly, we find that structural aneuploidies produced from segregation errors trigger p53 activation, and hence their propagation is limited to p53-deficient cells. In contrast, we show that not all whole-chromosome aneuploidies trigger p53 activation and that at least a subset of these is tolerated in p53-proficient backgrounds.

RESULTS

Induction of Chromosome Aneuploidies

To study the effects of induced aneuploidy, we selected a stable, near-diploid, non-transformed human cell line, RPE-1, and included an RPE-1-derived cell line with a stable short hairpin RNA (shRNA)-mediated knockdown of p53 (Figures S1A and S1B). Previous systems to induce aneuploidy mostly involved treatments with drugs that block cells in mitosis, followed by drug washout to allow mitotic progression with increased numbers of faulty attached chromosomes (Crasta et al., 2012; Janssen et al., 2011; Thompson and Compton, 2010). However, it was previously shown that prolonged mitotic timing results in a p53-dependent G1 arrest (Uetake and Sluder, 2010). To prevent a mitotic delay, we interfered with the mitotic checkpoint as a way to induce aneuploidy. Treatment with an MPS1 inhibitor at a dose that fully inactivates the mitotic checkpoint (Koch et al.,

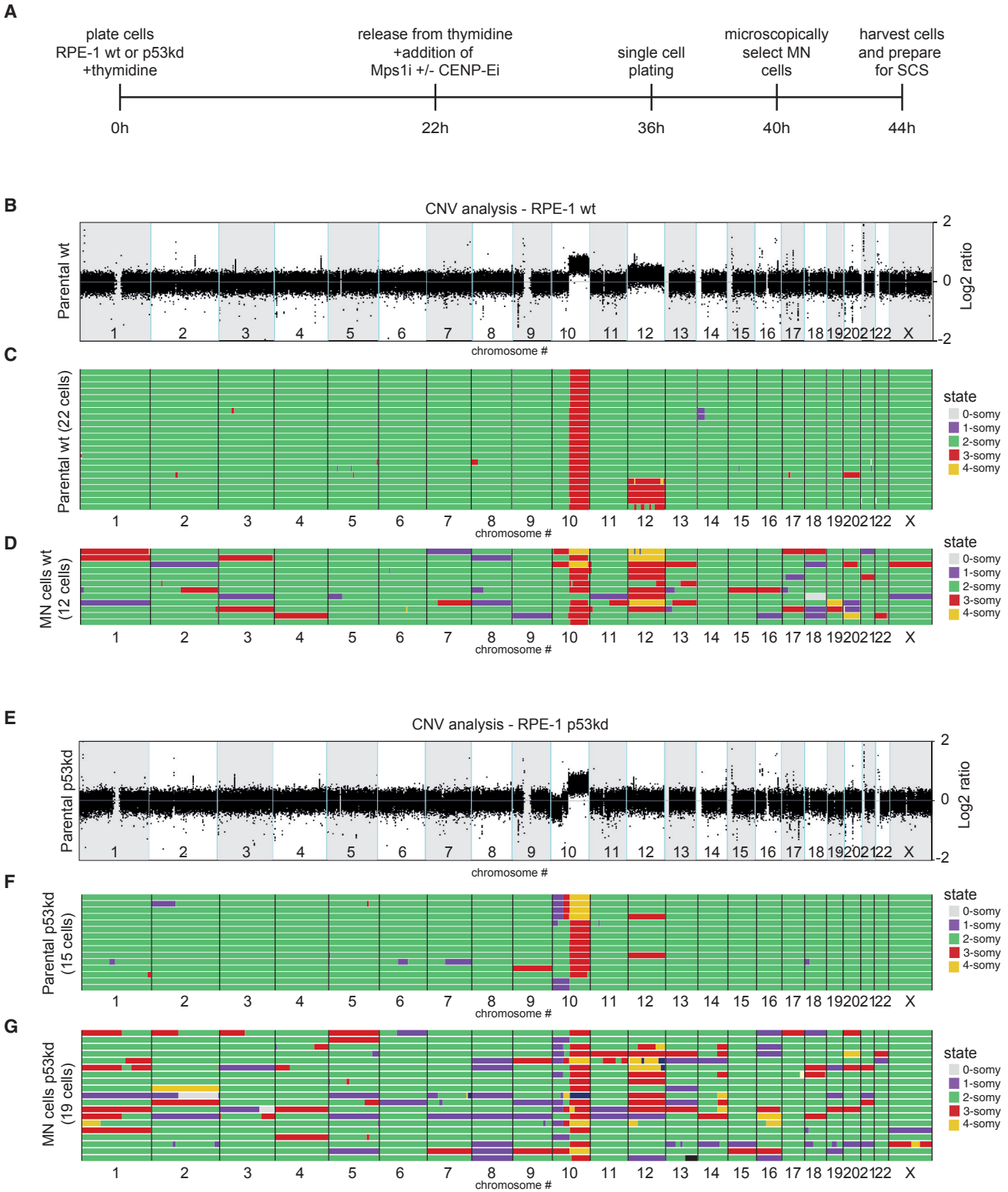

Figure 1. Induced Aneuploidy Using MPS1i/CENP-Ei Combinatory Treatment

(A) Schematic overview of the experimental setup to harvest single cells after induced chromosome missegregation.

(B) Genome-wide chromosome copy number profile of RPE-1 WT cells as determined by CNV sequencing (CNV-seq).

(legend continued on next page)

2016) indeed resulted in massive chromosome missegregations (92% of cell divisions) (Figures S2A–S2C), often accompanied by the formation of micronuclei (Figures S2D and S2E). However, using this dose, we observed a large number of chromosome bridges, previously shown to be susceptible to breakage and formation of structural aneuploidies (Janssen et al., 2011). Because we also wanted to study the effects of whole-chromosome aneuploidies, we set out to increase the amount of whole-chromosome missegregations. To this end, we combined a low dose of the MPS1 inhibitor (NMS-P715) with an allosteric inhibitor of the CENP-E kinesin (GSK923295) (Qian et al., 2010). The concept of co-inhibition of CENP-E and the spindle assembly checkpoint (SAC) has been explored before (Bennett et al., 2015; Ohashi et al., 2015), but here we adjusted the system to induce chromosome aneuploidies without delaying cells in mitosis. CENP-E inhibition causes chromosomes to remain at the spindle poles (1.7 ± 1.11 chromosomes per pole on average, as determined by centromere staining). Combining a CENP-E inhibitor with a low dose of MPS1 inhibitor resulted in a large amount of polar chromosome missegregations as compared with treatment with MPS1 inhibitor alone (~55% versus ~17%; see Figures S2C–S2E). Importantly, mitotic duration using the combination of drugs is comparable with that of untreated cells (Figure S2F), and only a subset of missegregating chromosomes end up in a micronucleus (Figure S2E). The majority of these micronuclei contains only one chromatid, a subset contains no centromere (indicating that they contain broken chromosome fragments), and another subset contains two centromeres (likely derived from a polar chromosome pair) (Figure S2G).

To reveal the aneuploidies we induce with our system, we used single-cell sequencing to determine the copy number variation per cell (Bakker et al., 2016; van den Bos et al., 2016). First, we performed single-cell plating of cells that were treated overnight with the combination of CENP-E inhibitor and MPS1 inhibitor (Figure 1A). Because not all cells displayed a missegregation event upon treatment (Figure S2C), we decided to select only cells that harbored a micronucleus as a marker for a missegregation event. Untreated cells were used as a control. Micro-amplifications or abnormalities around regions with repetitive sequences such as centromeres were not counted as genuine events, as they potentially are a consequence of incorrect "calling" due to noise or low read counts. Both copy number variation (CNV) analysis and single-cell sequencing analysis showed that the parental, untreated RPE-1 wild-type cells harbor a gain of the q-arm of chromosome 10 (Figures 1B and 1C). This gain is a result of a known unbalanced translocation of chromosome 10q to the X chromosome (Janssen et al., 2011; ATCC). Furthermore, we find a subset of cells containing three copies of chromosome 12. Although the origin of this event is unclear, it has been previously described (Zhang et al., 2015) and is likely a spontaneous, early event. Because these abnormalities are already present in the parental cells, we do not score these as de novo aneuploidies. A gain of chromosome 20 could be observed in 1 of 22 cells analyzed, indicating that RPE-1 cells display a basal but low level of chromosome instability. As expected, the micronucleated cells harvested after drug treatment displayed a large number of chromosome imbalances. As many as 84% had acquired de novo aneuploidies, and 75% of all cells displayed aneuploidies that involved whole chromosomes (i.e., numerical aneuploidies) (Figure 1D). Gains and losses of chromosomes fragments were found in 42% of the cells and are likely a result of chromosomes that were broken after anaphase (i.e., structural aneuploidies). Similar to the wild-type (WT) cells, the p53kd cells also displayed an occasional gain of chromosome 12 and the gain of the 10q arm. In addition, a subset of cells displayed a more complex profile of chromosome 10, where an additional loss of a part of the chromosome 10p arm could be observed, an event that could also be detected in the CNV analysis (Figures 1E and 1F). Importantly, loss of p53 resulted in a more unstable karyotype as multiple gains and losses could already be observed before treatment (Figure 1F), an observation consistent with what was previously seen in organoids (Drost et al., 2015). The p53kd micronucleated cells resulting from the treatment with the drug combination displayed an additional, severe increase in the amount of chromosome imbalances, comparable with the effects seen in RPE-1 WT cells (95% had acquired de novo aneuploidies). Ninety percent of all cells displayed aneuploidies that involved whole-chromosome imbalances, and 68% of the cells displayed structural imbalances (Figure 1G). It is important to note that most micronuclei-containing cells must have additional aneuploidies in the mother nucleus, because the majority of cells display multiple gains and losses (Figures 1D and 1G), while the micronucleus on average contained only one chromatid (Figure S2G). Taken together, these data demonstrate that combining CENP-E and MPS1 inhibitors is an efficient strategy to induce both whole-chromosome and structural chromosome missegregations without inducing a mitotic delay.

Aneuploidy Does Not Invariably Trigger a p53-Dependent Cell-Cycle Arrest

To determine the effect of induced aneuploidy on cell fate, we performed live cell imaging of cells in the presence of CENP-E inhibitor and MPS1 inhibitor to induce a missegregation event. After 10 hr, drugs were removed from the cells, and we imaged the cells for an additional 82 hr to determine the capacity of these cells to enter a second mitosis (see Figure 2A for experimental setup). To be consistent with our single-cell sequencing analysis, we traced only cells that contained a micronucleus after the first division. We found that the majority of micronucleated p53kd cells underwent a second mitosis (Figure 2B). Strikingly, we found that a large proportion of micronucleated WT cells

(C) Genome-wide chromosome copy number profile of RPE-1 WT cells as determined by single-cell sequencing using the AneuFinder pipeline as described previously (Bakker et al., 2016; van den Bos et al., 2016). Each row represents a single cell, with chromosomes plotted as columns. Different colors are used to depict copy number state.

(D) Genome-wide copy number profile of micronucleated RPE-1 WT cells after overnight treatment with the combination of CENP-E inhibitor (50 nM) and MPS1 inhibitor (480 nM) as determined by single-cell sequencing.

(E–G) Same as (B), (C), and (D) but for RPE-1 p53kd cells.

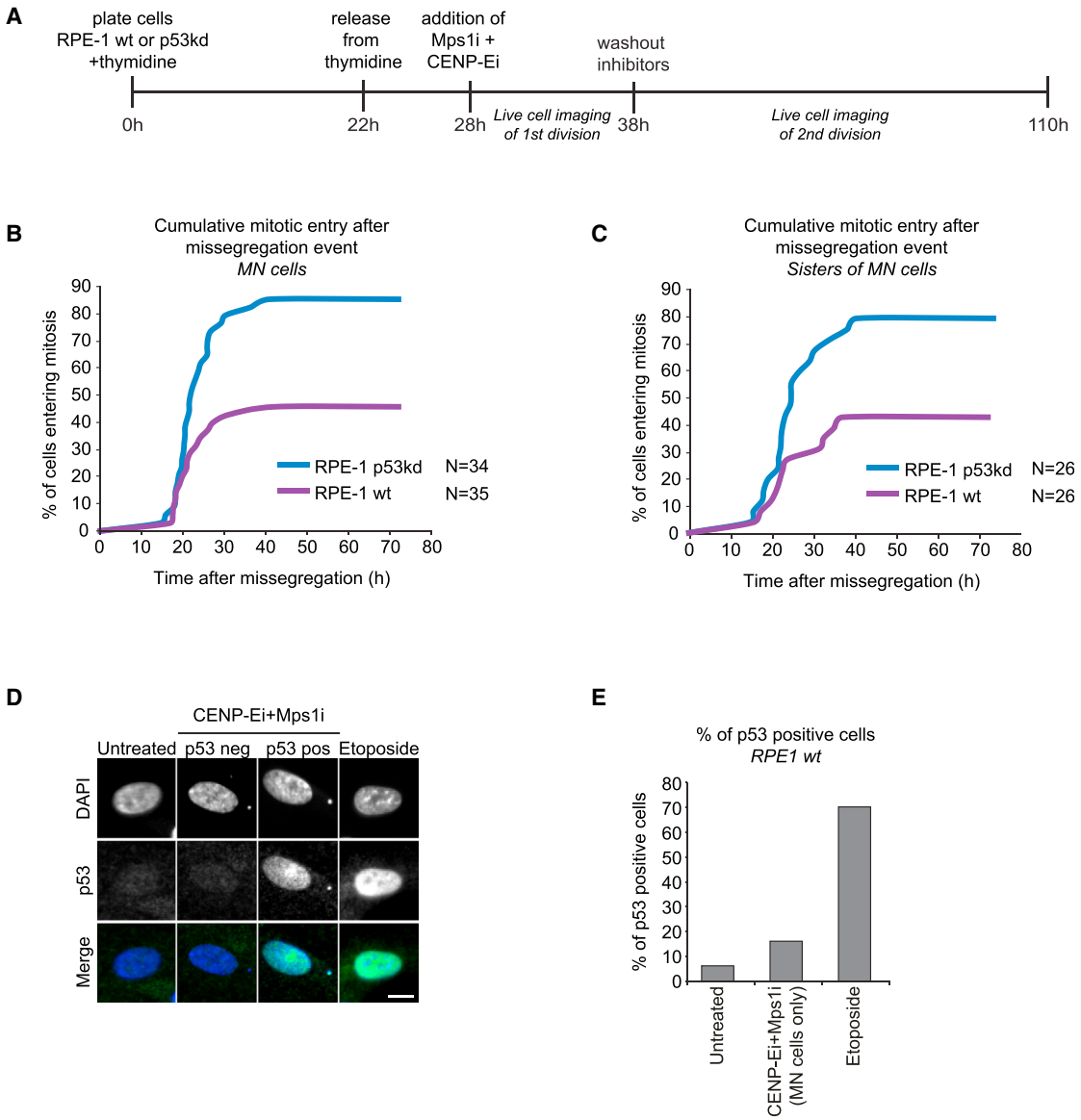

Figure 2. Aneuploidy Does Not Invariably Trigger a p53-Dependent Cell-Cycle Arrest

(A) Experimental setup to trace micronucleated cells for their capability to enter a subsequent mitosis.

(B) Cumulative mitotic entry of RPE-1 WT and RPE-1 p53kd cells stably expressing H2B-Dendra2 that were treated with the combination of CENP-E inhibitor (50 nM) and MPS1 inhibitor (480 nM). Time point 0 represents time of the missegregation event in the presence of drugs. Only cells that contained micronuclei and that could be traced for at least 52 hr were included. A total of 35 WT and 34 p53kd cells were analyzed. Images were taken every 10 min.

(C) Cells were treated as in (B). Only the sisters of micronucleated cells that did not contain micronuclei themselves and that could be traced for at least 52 hr were included. A total of 26 WT and 26 p53kd cells were analyzed from three independent experiments.

(D) Representative images of RPE-1 WT cells used to determine the percentage of p53 positivity by immunofluorescence staining. Thymidine-released cells were treated with the indicated inhibitors overnight. Inhibitors were washed out in the morning, and cells were fixed and stained 24 hr post-washout. As a control, cells were either left untreated or were treated for 3 hr with Etoposide (10 μM). The scale bar represents 10 μm.

(E) Quantification of p53-positive cells from cells in (D). Cells were identified on the basis of DAPI, and a pre-set threshold was used to determine p53 positivity. One hundred cells were analyzed in the untreated and etoposide condition and 148 MN cells treated with MPS1 and CENP-E inhibitors.

(~40%) also divided again (Figure 2B), even though >80% of these cells had become aneuploid (Figure 1D). This clearly indicates that p53 does not invariably arrests all aneuploid cells in response to a missegregation event. A similar effect could be seen on the sisters of the micronucleated cells (Figure 2C), indicating that this effect is not specific to micronucleated cells but applies to aneuploid cells in general. In line with that, we observed upregulation of p53 in only a fraction (~16%) of fixed post-anaphase micronucleated cells (Figures 2D and 2E). This fraction is lower than would be expected from our live cell

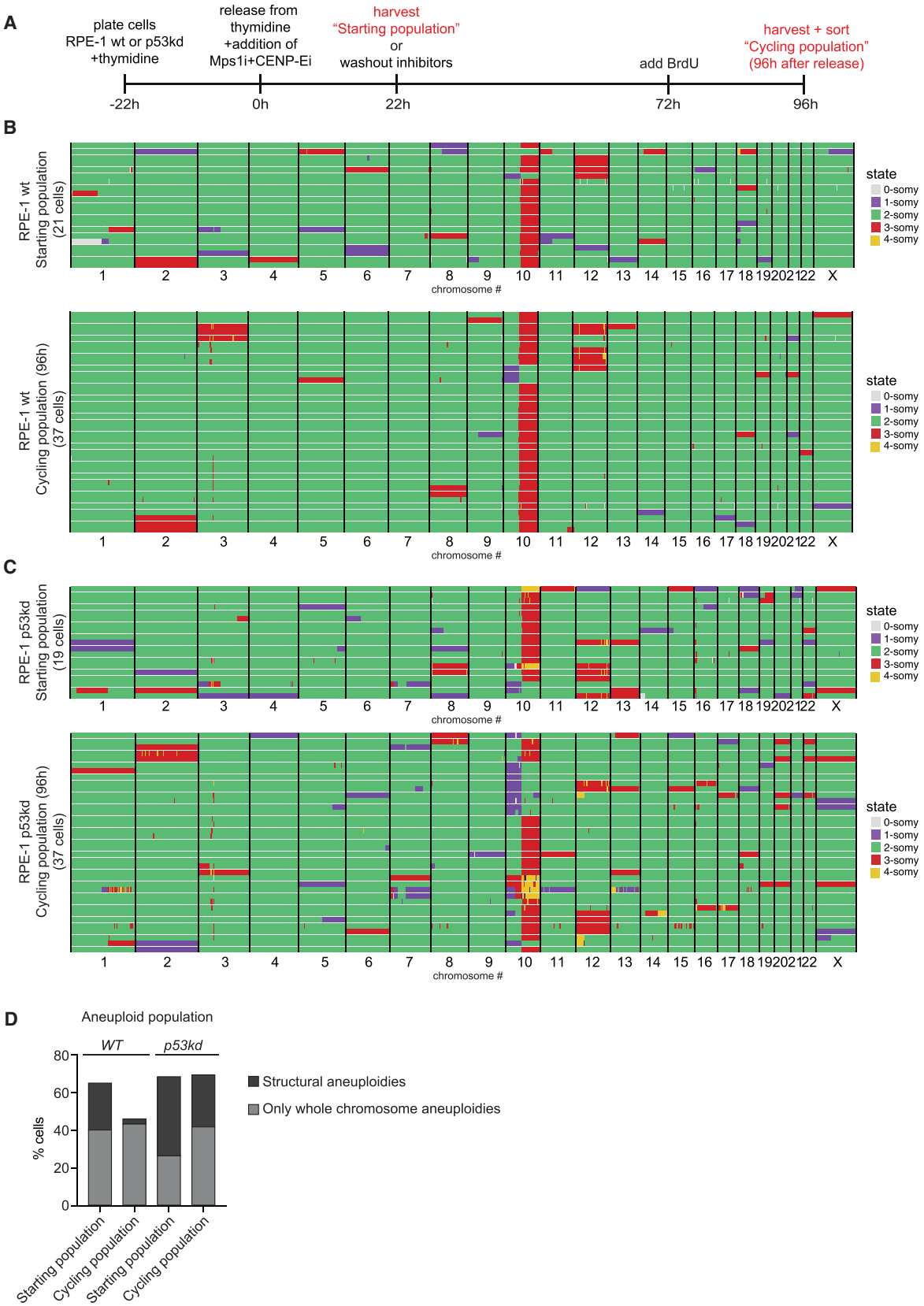

(legend on next page)

experiments, because approximately 40% of micronucleated cells arrest in a p53-dependent manner (Figures 2B and 2C). However, because quantification of p53 is performed at a fixed time point, this may lead to a underestimation of the fraction of cells that activates p53, as p53 is known to oscillate in response to DNA damage (Batchelor et al., 2011). Taken together, our data clearly shows that aneuploidy does not always result in p53 activation.

Propagation of Structural Aneuploidies Is Limited to p53-Deficient Cells

We next determined which type of aneuploidies could be propagated in p53-proficient versus p53-deficient cells. To this end, we first evaluated the overall extent of aneuploidy obtained by MPS1i/CENP-Ei treatment (referred to as the "starting population") and compared this with the extent of aneuploidy in cells that were still actively cycling 3 days post-MPS1i/CENP-Ei treatment (on the basis of BrdU incorporation; referred to as "cycling population") (see Figure 3A for experimental setup). Single-cell sequencing of the starting population revealed that an equal fraction of RPE-1 WT and p53kd cells became aneuploid upon the combinatory treatment (66.7% and 68.4%, respectively) (Figures 3B and 3C, top, and Figure 3D) but that the p53kd cells contained slightly more numerical and structural chromosomal alterations per cell, consistent with our previous results (Figures 1D and 1G). Importantly, the extent of aneuploidy decreased significantly in the cycling WT RPE-1 population but not in the p53kd RPE-1 cells (Figures 3B and 3C, bottom, and Figure 3D). Remarkably, whole-chromosome aneuploidies appeared to be quite well tolerated in both settings, whereas structural aneuploidies could hardly be observed in WT cells that were still proliferating 3 days post-treatment (Figure 3D). This indicates that tolerance toward the structural aneuploidies we induce by combined CENP-E/MPS1 inhibition is strongly influenced by the p53 status of the cell.

Because we observed that aneuploid cells were still proliferating after 3 days, we reasoned that we should be able to generate full aneuploid clones, both in WT and p53kd RPE-1 cells. Importantly, tracing of the subsequent divisions of single cells over a multi-week time course (Figure S3A) showed that only 23% of the untreated single RPE-1 WT cells had the ability to grow out to a full clone, indicating that the proliferative capacity of RPE-1 WT cells is severely hampered when plated as single cells (Figure S3B). Micronucleated RPE-1 WT cells showed an even worse outcome, as the majority of cells did not divide at all or stopped dividing after one or two cell divisions (Figure S3B). However, two cells (1% of the starting population) continued to divide over the whole duration of the experiment and grew into full colonies (clones B18 and F12). To increase the clonal outgrowth of single-cell micronucleated WT RPE-1 cells, we removed the synchronization step and performed a transient depletion of p53 by small interfering RNA (siRNA) transfection 24 hr prior to the experiment. This approach notably increased the success of single-cell outgrowth of untreated WT cells as well as of the micronucleated WT cells, resulting in three full colonies (clones B22, A11, and I18, 6% of the starting population) (Figure S3C). In parallel, we performed similar experiments in the RPE-1 p53kd cells, which tolerated single-cell plating better (Figure S3D, left). Also, outgrowth of single micronucleated p53kd cells was more effective with 17% growing into full clones (Figure S3D, right).

To determine the exact ploidy of the clones that grew out from the single micronucleated cells, we performed CNV analysis. In the WT background, 3 clones had a similar ploidy as the WT parentals, whereas 2 clones displayed a whole-chromosome aneuploidy: a trisomy of chromosome 6 in clone A11 and a monosomy of chromosome 10 in clone I18 (Figure 4A). Interestingly, all clones were still p53 proficient as cell proliferation was blocked by Nutlin-3 (Figure S4; for technical reasons, clone A11 was lost and could therefore not be tested for Nutlin-3 sensitivity). Interestingly, in the clones derived from the p53kd cells, more severe aneuploidies could be observed (Figure 4B), with only 2 clones displaying the parental karyotype (clones K14 and E8). In contrast, the other 12 clones displayed either only numerical (clones C23, O8, D12, and I21), only structural (clone O9), or a combination of numerical and structural changes (clones F9, H21, E18, F13, I20, F20, and F6) (Figure 4B, right). These results imply that whole-chromosome aneuploidies can be tolerated in p53-proficient cells, whereas the propagation of structural aneuploidies is restricted to p53-deficient backgrounds.

DISCUSSION

p53 Does Not Sense Aneuploidy Per Se

Although aneuploidy induced by SAC deficiency is lethal in mouse embryonic fibroblasts (MEFs) (at least in part) because of p53-induced apoptosis (Burds et al., 2005), stable aneuploid MEFs do not show elevated p53 levels (Tang et al., 2011). Also, SAC deficiency is tolerated in the murine interfollicular epidermis, suggestive of limited p53 activation (Foijer et al., 2013). Nonetheless, a p38/p53-dependent cell-cycle arrest has been reported in response to chromosome missegregation events in cell culture (Thompson and Compton, 2010), and elevated levels of p53 have been observed at least in the CNS of Down syndrome patients (Liao et al., 2012). Thus, whether p53 can sense aneuploidy per se has remained controversial. Here, we set up a system to induce both numerical and structural aneuploidies. Using this system, we found that p53 is

Figure 3. Propagation of Structural Aneuploidies Is Limited to p53-Deficient Cells

(A) Schematic overview of the experimental setup to sequence single cells directly after a whole-chromosome missegregation event as well as cells that were still actively cycling 96 hr post-treatment.

(B) Genome-wide chromosome copy number profile of RPE-1 WT cells as determined by single-cell sequencing as in Figure 1. Each row represents a single cell, with chromosomes plotted as columns. Different colors are used to depict copy number state.

(C) Same as in (B) but for RPE-1 p53kd cells.

(D) Percentage of cells from (B) and (C) harboring only whole-chromosome aneuploidies or cells harboring structural aneuploidies (with or without additional whole-chromosome aneuploidies) were determined per condition.

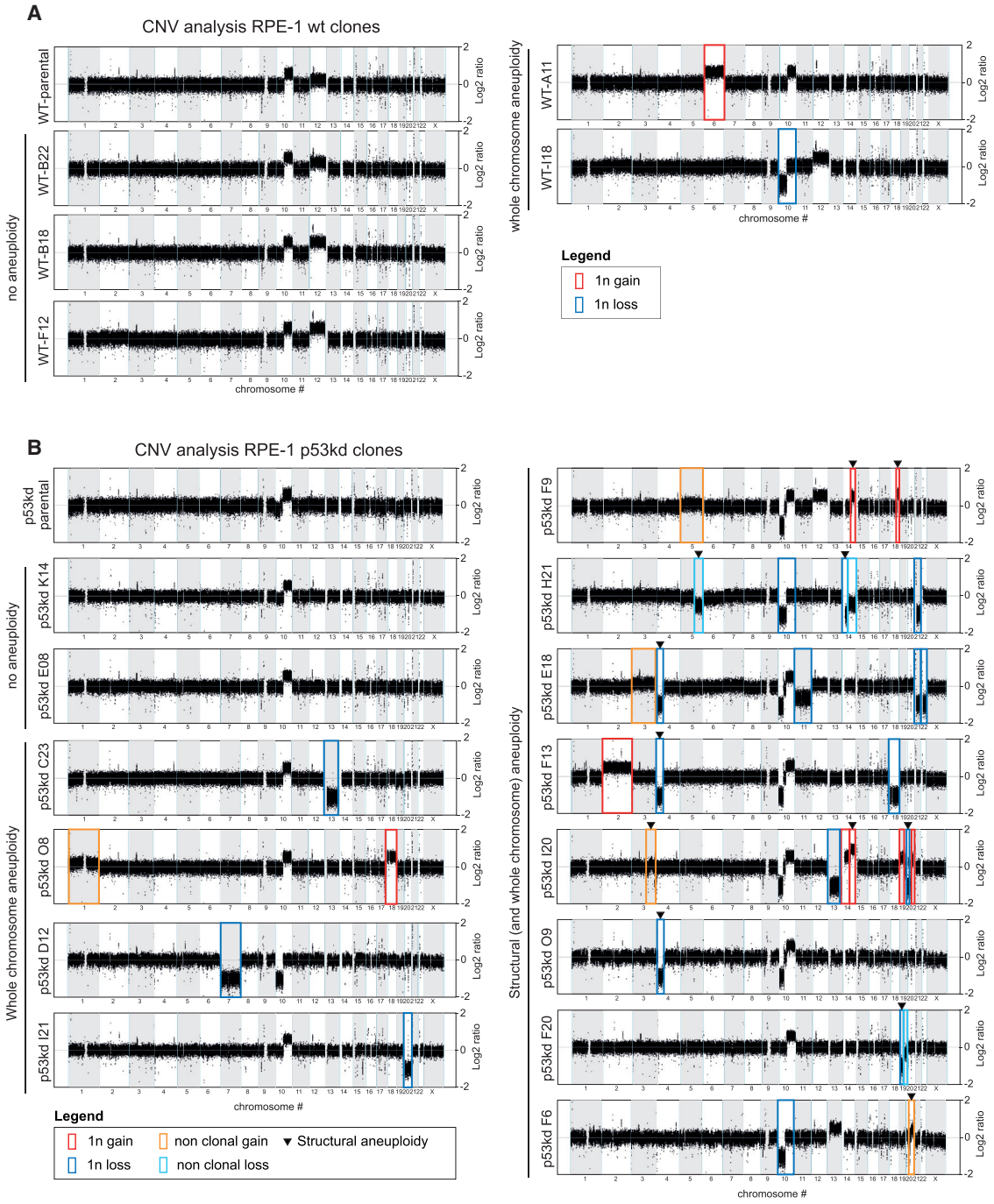

Figure 4. Characterization of Aneuploid Clones

(A) Genome-wide chromosome copy number profile as determined by CNV-seq of five RPE-1 WT clones and their parental cell line. Chromosome gains are depicted in red and losses in blue. Alteration of chromosomes 10 and 12 that are already present in the parental cells are not highlighted.

(B) Genome-wide chromosome copy number profile as determined by CNV-seq of 14 RPE-1 p53kd clones and their parental cell line. Chromosome gains are depicted in red and losses in blue. Gains or losses that are less than what would be expected from a monosomic event (a $\log_2$ ratio > -1) or from a trisomic event (a $\log_2$ ratio < 0.5) might reflect non-full clonal losses or gains and are depicted in orange and light blue, respectively.

upregulated in only a fraction of the non-transformed, p53-proficient human cells after a missegregation event and that a large fraction of cells will continue to divide after a missegregation event. Moreover, we found that even multiple days after the missegregation event, p53-proficient cells can be observed that are actively proliferating in the presence of whole-chromosome

imbalances. Finally, we were able to generate stable p53-proficient cell clones harboring a whole-chromosome aneuploidy. These results suggest that p53 is not always activated in response to aneuploidy, and therefore whole-chromosome imbalances can be stably propagated in p53-proficient cells.

Mild Whole-Chromosome Aneuploidies Can Be Tolerated and Propagated in a p53-Proficient Background

Our data show that at least a subset of whole-chromosome aneuploidies can be tolerated in p53-proficient cells. However, the fact that the total amount of whole-chromosome abnormalities per cell drops significantly in the proliferating population of WT cells compared with the p53-deficient cells after 3 days suggests that whole-chromosome aneuploidy can sometimes activate p53 to the extent that does prevent further proliferation. Likely, the degree of aneuploidy is an important determinant here. As has been shown before, the higher the level of aneuploidy, the more cellular imbalances occur, leading to increased levels of cellular stress (Torres et al., 2007). Possibly, when the level of stress exceeds a certain threshold, p53 becomes activated to levels that prevent proliferation. Alternatively, particular whole-chromosome imbalances may be not tolerated because they could lead to perturbations in very specific, essential cellular processes.

Propagation of Structural Aneuploidies Is Limited to p53-Deficient Cells

By single-cell sequencing of actively proliferating aneuploid cells (Figure 3), we revealed that p53 prevents cells that harbor structural aneuploidies to proliferate. We have previously shown that structural chromosomal aberrations can result from chromosomal missegregations that induce chromosome breakage (Janssen et al., 2011). As broken chromosomes activate the DNA damage checkpoint through the activation of ATM, it is likely that p53 gets activated in response to these types of segregation errors. Indeed, although structural aneuploidies are induced to the same extent in both p53-proficient and p53-deficient cells, propagation of these structural aneuploidies is limited to the p53-deficient cells (Figures 3 and 4). Interestingly, although numbers are small, single-cell sequencing of aneuploid cells indicates that chromosome breakage occurs more often in large chromosomes, suggesting that larger chromosomes are more likely to break when the SAC is compromised compared with the smaller chromosomes. This may reflect a selective effect on larger chromosomes or may simply be a consequence of increased size.

Our results suggest that DNA breaks induced by chromosome missegregation events result in a permanent cell-cycle arrest in p53-proficient cells. However, it is important to point out that the WT RPE-1 cells stably propagate a structural aneuploidy, namely, the translocation of 10q to chromosome X, indicating that structural aneuploidies per se do not prohibit proliferation of p53-proficient cells. This suggests that the manner in which the structural aneuploidy is generated will determine if it can be propagated in a p53-proficient setting and that structural aneuploidies that arose through a different mechanism, such as a recombination event, can be propagated in p53-proficient cells. Taken together, we find that a whole-chromosome imbalance per se is not sufficient to induce a p53-dependent cell-cycle arrest and that at least a subset of whole-chromosome aneuploidies can be tolerated and propagated. In contrast, structural aneuploidies that are produced by chromosome missegregation are solely tolerated and propagated in p53-deficient cells.

EXPERIMENTAL PROCEDURES

Cell Culture and Reagents

hTERT-immortalized RPE-1 were from ATCC. RPE-1 p53kd cells were generated by transduction with pRetroSuper-p53 (with the shRNA sequence 5′-CTACATGTGTAACAGTTCC-3′) and selected with Nutlin-3 for functional loss of p53. Cell culture and synchronization procedures were described previously (Janssen et al., 2011). Inhibitors were all dissolved in DMSO and were used at the following concentrations: proTAME, 20 μM; GSK923295, 50 nM; NMS-P715, 480 nM; Cpd-5, 200 nM; and Nutlin3a, 10 μM.

Time-Lapse Imaging

For live-cell imaging, cells were grown in Lab-Tek II chambered coverglass (Thermo Fisher Scientific). Imaging was performed as previously described (Koch et al., 2016).

siRNA Transfection

ON-TARGETplus SMARTpool siRNA targeting p53 (Thermo Fisher Scientific) was transfected using RNAiMAX (Life Technologies) according to the manufacturer's protocol in a final concentration of 20 nM, 24 hr before the start of the experiment.

Immunofluorescence

Cells were grown on 10-mm glass coverslips and fixed in 3.7% formaldehyde/0.5% Triton X-100 in PBS for 15 min at room temperature. Primary antibody for p53 (sc-126; Santa Cruz) was incubated at 4°C overnight, and secondary antibody (Alexa Fluor 488; Molecular Probes) was incubated for 2 hr at room temperature, both dissolved in PBS 0.1% Tween. DAPI was added to all samples before mounting using Vectashield mounting fluid (Vector Laboratories). Images were acquired on a DeltaVision Elite microscope (Applied Precision), taking 200-nm z stacks with a PlanApo N 60×/NA 1.42 objective (Olympus) and a Coolsnap HQ2 camera (Photometrics). Images were analyzed after deconvolution using SoftWoRx (Applied Precision). Figures are maximum-intensity projection of entire cells. Brightness and contrast were adjusted with Photoshop 6.0 (Adobe).

Copy Number Analysis

For a detailed description of the methods used for CNV and single-cell sequencing, see Supplemental Experimental Procedures.

ACCESSION NUMBERS

The accession numbers for the single-cell sequencing and CNV data reported in this paper are ENA: PRJEB20826 and SRA: PRJNA386471, respectively.

SUPPLEMENTAL INFORMATION

Supplemental Information includes Supplemental Experimental Procedures and four figures and can be found with this article online at http://dx.doi.org/10.1016/j.celrep.2017.05.055.

AUTHOR CONTRIBUTIONS

M.S., J.A.R., and R.H.M. conceptualized the study. M.S., J.A.R., B.B., and D.C.J.S. conducted experiments. B.B. analyzed the single-cell sequencing data. F.F. and P.M.L. provided resources and input on the project. M.S., J.A.R., and R.H.M. wrote the manuscript.

ACKNOWLEDGMENTS

This research was funded by the Marie Curie Initial Training Network Project PLOIDYNET (FP7-PEOPLE-2013 and 607722), the Gravitation Program (Cancer Genomics Center, CGC.nl, project #58588) to R.H.M.; and the Dutch Cancer Foundation (NKI-2015-7832) to R.H.M. and J.A.R. We thank all Medema, Rowland, and Jacobs lab members for helpful discussions and J. Kuiken and R. Beijersbergen for the RPE-1 p53kd cell line. We thank the Genomics Core Facility of the Netherlands Cancer Institute for sample preparation, data acquisition, and analysis of CNV experiments.

Received: November 16, 2016
Revised: May 3, 2017
Accepted: May 17, 2017
Published: June 20, 2017

REFERENCES

Bakker, B., Taudt, A., Belderbos, M.E., Porubský, D., Spierings, D.C.J., de Jong, T.V., Halsema, N., Kazemier, H.G., Hoekstra-Wakker, K., Bradley, A., et al. (2016). Single-cell sequencing reveals karyotype heterogeneity in murine and human malignancies. Genome Biol. *17*, 115.

Batchelor, E., Loewer, A., Mock, C., and Lahav, G. (2011). Stimulus-dependent dynamics of p53 in single cells. Mol. Syst. Biol. *7*, 488.

Bennett, A., Bechi, B., Tighe, A., Thompson, S., Procter, D.J., and Taylor, S.S. (2015). Cenp-E inhibitor GSK923295: novel synthetic route and use as a tool to generate aneuploidy. Oncotarget *6*, 20921–20932.

Burds, A.A., Lutum, A.S., and Sorger, P.K. (2005). Generating chromosome instability through the simultaneous deletion of Mad2 and p53. Proc. Natl. Acad. Sci. U S A *102*, 11296–11301.

Crasta, K., Ganem, N.J., Dagher, R., Lantermann, A.B., Ivanova, E.V., Pan, Y., Nezi, L., Protopopov, A., Chowdhury, D., and Pellman, D. (2012). DNA breaks and chromosome pulverization from errors in mitosis. Nature *482*, 53–58.

Drost, J., van Jaarsveld, R.H., Ponsioen, B., Zimberlin, C., van Boxtel, R., Buijs, A., Sachs, N., Overmeer, R.M., Offerhaus, G.J., Begthel, H., et al. (2015). Sequential cancer mutations in cultured human intestinal stem cells. Nature *521*, 43–47.

Foijer, F., DiTommaso, T., Donati, G., Hautaviita, K., Xie, S.Z., Heath, E., Smyth, I., Watt, F.M., Sorger, P.K., and Bradley, A. (2013). Spindle checkpoint deficiency is tolerated by murine epidermal cells but not hair follicle stem cells. Proc. Natl. Acad. Sci. U S A *110*, 2928–2933.

Gordon, D.J., Resio, B., and Pellman, D. (2012). Causes and consequences of aneuploidy in cancer. Nat. Rev. Genet. *13*, 189–203.

Holland, A.J., and Cleveland, D.W. (2009). Boveri revisited: chromosomal instability, aneuploidy and tumorigenesis. Nat. Rev. Mol. Cell Biol. *10*, 478–487.

Janssen, A., van der Burg, M., Szuhai, K., Kops, G.J.P.L., and Medema, R.H. (2011). Chromosome segregation errors as a cause of DNA damage and structural chromosome aberrations. Science *333*, 1895–1898.

Koch, A., Maia, A., Janssen, A., and Medema, R.H. (2016). Molecular basis underlying resistance to Mps1/TTK inhibitors. Oncogene *35*, 2518–2528.

Li, M., Fang, X., Baker, D.J., Guo, L., Gao, X., Wei, Z., Han, S., van Deursen, J.M., and Zhang, P. (2010). The ATM-p53 pathway suppresses aneuploidy-induced tumorigenesis. Proc. Natl. Acad. Sci. U S A *107*, 14188–14193.

Liao, J.-M., Zhou, X., Zhang, Y., and Lu, H. (2012). MiR-1246: a new link of the p53 family with cancer and Down syndrome. Cell Cycle *11*, 2624–2630.

Ohashi, A., Ohori, M., Iwai, K., Nakayama, Y., Nambu, T., Morishita, D., Kawamoto, T., Miyamoto, M., Hirayama, T., Okaniwa, M., et al. (2015). Aneuploidy generates proteotoxic stress and DNA damage concurrently with p53-mediated post-mitotic apoptosis in SAC-impaired cells. Nat. Commun. *6*, 7668.

Qian, X., McDonald, A., Zhou, H.-J., Adams, N.D., Parrish, C.A., Duffy, K.J., Fitch, D.M., Tedesco, R., Ashcraft, L.W., Yao, B., et al. (2010). Discovery of the first potent and selective inhibitor of centromere-associated protein E: GSK923295. ACS Med. Chem. Lett. *1*, 30–34.

Santaguida, S., and Amon, A. (2015). Short- and long-term effects of chromosome mis-segregation and aneuploidy. Nat. Rev. Mol. Cell Biol. *16*, 473–485.

Segal, D.J., and McCoy, E.E. (1974). Studies on Down's syndrome in tissue culture. I. Growth rates and protein contents of fibroblast cultures. J. Cell Physiol. *83*, 85–90.

Tang, Y.-C., Williams, B.R., Siegel, J.J., and Amon, A. (2011). Identification of aneuploidy-selective antiproliferation compounds. Cell *144*, 499–512.

Thompson, S.L., and Compton, D.A. (2010). Proliferation of aneuploid human cells is limited by a p53-dependent mechanism. J. Cell Biol. *188*, 369–381.

Torres, E.M., Sokolsky, T., Tucker, C.M., Chan, L.Y., Boselli, M., Dunham, M.J., and Amon, A. (2007). Effects of aneuploidy on cellular physiology and cell division in haploid yeast. Science *317*, 916–924.

Uetake, Y., and Sluder, G. (2010). Prolonged prometaphase blocks daughter cell proliferation despite normal completion of mitosis. Curr. Biol. *20*, 1666–1671.

van den Bos, H., Spierings, D.C.J., Taudt, A.S., Bakker, B., Porubský, D., Falconer, E., Novoa, C., Halsema, N., Kazemier, H.G., Hoekstra-Wakker, K., et al. (2016). Single-cell whole genome sequencing reveals no evidence for common aneuploidy in normal and Alzheimer's disease neurons. Genome Biol. *17*, 116.

Williams, B.R., Prabhu, V.R., Hunter, K.E., Glazier, C.M., Whittaker, C.A., Housman, D.E., and Amon, A. (2008). Aneuploidy affects proliferation and spontaneous immortalization in mammalian cells. Science *322*, 703–709.

Zhang, C.-Z., Spektor, A., Cornils, H., Francis, J.M., Jackson, E.K., Liu, S., Meyerson, M., and Pellman, D. (2015). Chromothripsis from DNA damage in micronuclei. Nature *522*, 179–184.